Defects and Lattice Instability in Doped Lead-Based Perovskite Antiferroelectrics: Revisited

Dariusz Kajewski

Institute of Physics, Univeristy of Silesia, ul. 75 Pułku Piechoty 1, 41-500 Chorzów, Poland;
dariusz.kajewski@us.edu.pl

Abstract: This paper is a summary of earlier results that have been completed with recent investigations on the nature and sequence of phase transitions evolving in the antiferroelectric $PbZrO_3$ single crystals doped with niobium and $Pb(Zr_{0.70}Ti_{0.30})O_3$ ceramics doped with different concentration of Bi_2O_3. It was found that these crystals undergo new phase transitions never observed before. To investigate all phase transitions, different experimental methods were used to characterize the crystal properties. Temperature and time dependencies have been tentatively measured in a wide range, including a region above T_c, where precursor dynamics is observed in the form of non-centrosymmetric regions existing locally in crystal lattices. Also, coexistence of antiferroelectric phase and one of the intermediate phases could be observed in a wide temperature range. The phase transition mechanism in $PbZrO_3$ is discussed, taking into account the local breaking of the crystal symmetry above T_c and the defects of crystal lattices, i.e., those generated during crystal growth, and intentionally introduced by preheating in a vacuum or doping with hetero-valent dopant.

Keywords: lead zirconate; phase transitions; defects

---

1. Introduction

Ferroelectrics and antiferroelectrics with perovskite structure which contain oxygen octahedrons are of great interest to scientists not only because of their numerous applications, but also because of their versatile properties. Although many of them have been known for over 60 years and many theoretical and experimental works have already been reported, there is a range of newly discovered phenomena that remain unknown. They concern mainly lattice dynamics and type-of-phase transitions, i.e., whether they are of the order–disorder or displacement type [1]. In the literature, one can find contradictory experimental data supporting the mechanism associated with pure order–disorder or displacement type. However, investigations of macroscopic properties show characteristic phonon softening associated with displacement type transition, and studies of local properties support the order–disorder one [1–9]. Experiments concerning local properties also show the existence of polar clusters that appear far above T_c temperature. With the lowering of temperature, these regions increase in volume and eventually merge into the ferroelectric state below T_c [10]. Such scenario explains well the surprising occurrence of birefringence in $BaTiO_3$ single crystals above T_c, i.e., in the centrosymmetric phase that excludes birefringence altogether [11].

Polar regions (precursors) in the paraelectric phase of $BaTiO_3$ crystals have also been observed by means of other experimental methods, such as Brillouin light scattering. The appearance of these regions was correlated with the softening of longitudinal acoustic mode some 80 K above T_c [12]. This experiment proved that the origin of precursor appearance is mainly connected with (flexoelectric) interactions between the optic and acoustic phonon leading to the so-called lattice instabilities. It is worth noting that picosecond laser techniques were used to show that the size of polar regions increases

---

while transition is approached from the high temperature side [13]. Similar lattice instabilities were found in other crystals as $PbTiO_3$ [14], $PbHfO_3$ [15–17], or model antiferroelectric $PbZrO_3$ (PZO) [18].

The lead zirconate $PbZrO_3$ is particularly interesting, due to its antiferroelectric properties and due to the occurrence of ferroelectric properties just below T_c phase, also under the influence of even small electric fields [19–23]. Often the occurrence of this phase is associated with the presence of defects in lead and oxygen sublattices [24–28]. It is worth noting that mentioned defects do not influence the room temperature crystal structure. However, this could be stated only by standard X-ray diffraction methods which are not so sensitive for changes in oxygen ions positions. Recently, the nature of this phase was characterized by Brillouin light scattering method and described as the coexistence of paraelectric and antiferroelectric phases. At the same time, polar regions above T_c were detected [29]. Hence, it is worth noting that on the one hand the occurrence of the intermediate phase depends on crystal lattice defects, and on the other hand polar regions, according to the theory of Bussmann-Holder et al. [30], occur in centrosymmetric phase without any defects. This contradiction became the main motivation for investigations presented in this paper.

The purpose of research has been to determine the impact of crystal lattice defects, and their nature, on phase transitions and local symmetry breaking in crystals and ceramics based on $PbZrO_3$. Achieving such a goal can be divided into the following parts:

- Determination of the influence of defects generated under high vacuum conditions on phase transitions temperature in pure $PbZrO_3$ [31],
- Determination of the influence of donor dopant in the form of niobium on the lattice dynamics in $PbZrO_3$ crystal and breaking of local symmetry above T_c [32–36],
- Determination of the role of crystal surface and volume in dielectric properties of the $PbZrO_3$ crystal doped with niobium, in which defect segregation was generated by alternating electric field action [37].

Additionally, investigations will be presented concerning the presence of polar regions above and below T_c in $PbZr_{0.70}Ti_{0.30}O_3$ ceramics doped with bismuth [38].

2. Materials and Methods

Three types of materials were used in these investigations:

- Pure $PbZrO_3$ crystals obtained by high temperature spontaneous crystallization from solvent: the substrates in the form of PbO, B_2O_3, and $PbZrO_3$ ceramics were weighed in correct proportions and mixed together; the preparation of $PbZrO_3$ ceramics is described in detail in [23], while the exact process of crystal growth is described in [39]; crystals in the form of red plates were obtained; these crystals were deliberately defected by remaining for 15 min in high temperatures and under high vacuum (approximately 10^{-5} mbar) [31];
- $PbZrO_3$ crystals doped with niobium were obtained by two methods: the same as that used in growing crystals of pure $PbZrO_3$ and the other based on $PbZrO_3$ ceramics doped with niobium; the preparation of ceramics used for breeding is described in [40], while the preparation of crystals is described in [32]; crystals were in the form of red colored plates and bars; the latter method which used substrates consisting of oxides alone (without the use of ceramics) is described in [34]; the resulting crystals were plate-shaped and slightly yellow in color;
- $Pb(Zr_{0.70}Ti_{0.30})O_3$ ceramics doped with different concentration of Bi_2O_3; their preparation process is described in detail in [38].

Lead zirconate is a model antiferroelectric discovered in the 1950s [41]. It is one of the components of lead titanate zirconate (PZT), which is widely used as a piezoelectric or energy storage material [42,43]. A very interesting problem in $PbZrO_3$ appears to be the occurrence of both polar regions above T_c and the so-called intermediate phase [25,27,29,30], which under the influence of electric field has ferroelectric properties. Its nature has been discovered only recently [29] and has been described as coexistence

of phases (paraelectric and antiferroelectric) over a temperature range below T_c. The occurrence of this phase is explained in the literature by the presence of various types of technological pollution or lattice defects [44–47]. However, most of the research concerning the problem of lattice defects in PbZrO$_3$ relates to intentionally defective ceramics in a vacuum [26–28]. The use of ceramics, however, causes uncertainty as to the place, in which the defects developed under vacuum condition arise: whether it is grain boundary or grain interior. Thus, it seems difficult to find the answer concerning the impact of crystal lattice defects arising only in the crystal lattice of lead zirconate. Therefore, it seemed important to conduct similar investigations using crystals. Of importance is which sublattice defects are responsible for the occurrence of the intermediate phase, and what their type is. The issue was whether we must deal with vacancies or with change of oxidation states of the elements and even with the migration of atoms in the volume of crystal. This problem was presented in [31].

Another method of introducing controlled change in the number of defects is doping the base material with a hetero-valent dopant. In this case, niobium dopant was chosen due to the proven fact of stabilizing the intermediate phase in PbZrO$_3$ ceramics this dopant was responsible for [40]. As in the case of non-doped PbZrO$_3$ ceramics, it is difficult to determine how much the stress between ceramic grains is responsible for this state, and how niobium ions are embedded in crystalline structure. That is why single crystals are relevant to control the concentration and types of defects appearing due to doping. It should be remembered, however, that it is not easy to obtain good quality crystals doped with hetero-valent ions, due to the difficulty of incorporating such type of ion into the crystal lattice. Therefore, attempts were made to obtain crystals by two techniques to check whether crystal properties depend on the way in which there were obtained. The impact of dopant concentration on both pre-transient effects above T_c and on phase transitions mechanism is presented in [32–36]. In addition, PbZrO$_3$ crystal doped with niobium served as a crystal in which the migration of defects in the crystal lattice due to the action of strong alternating electric field was observed and appears to have a substantial impact on research of dielectric properties [37], particularly on the temperature dependence of maximum of permittivity that is defined by T_c value.

The third group concerns ceramics Pb(Zr$_{0.70}$Ti$_{0.30}$)O$_3$ (PZT 70/30) doped with different amount of Bi$_2$O$_3$. It is extremely difficult to obtain PZT crystals with high titanium content. Up to now it has been achieved only in two academic centers worldwide, but without dopant [48–53]. Because of that, it was decided to use PZT ceramics doped with Bi. Ceramics PZT 70/30 was selected since in the range of $0.3 \leq x \leq 0.4$ rhombohedral symmetry, as an effect of long-range interacting regions with local monoclinic symmetry induced by shifts of lead ions, has been ascertained [54]. This interesting phenomenon needs to be checked from the point of view of the role that lead atoms play in the PZT 70/30 structure and how they affect the dielectric properties of this compound. Bismuth ion, having ionic radius equal to 117 pm, only about 2 pm smaller than lead ion and of similar electronic structure, was chosen to substitute for lead. Such doping should make a slight change in the charge balance of the tested material, and should influence the symmetry of crystal structure. It should be due to defects in the Pb^{2+} sublattice created by introduction of bismuth ions with valence 3+ or due to compensation of charge carriers appearing as a result of lead vacancy appearance during technological process. The results of research on this compound are presented in [38].

The results presented in this report were obtained using the following experimental methods:

- capacitance and electrical conductivity measurements. It allowed determining temperature changes of permittivity and dielectric loss of tested materials. The measurements were performed with the use of an automated measurement system with impedance analyzer HP 4192A, multimeter HP 34401 and temperature controller Shiemaden FP23;
- birefringence (Δn) measurement as a function of temperature, using the method described in [55] and observations of domain structures using polarizing microscope and temperature heating stage THSE600 from Linkam;
- piezoelectric and electrostrictive properties as a function of temperature were determined using the measuring system described in [56];

- pyroelectric effect was observed by measurement of thermally stimulated depolarization currents using electrometer Keithley 6514, multimeter HP 34401 and temperature controller Shiemaden FP23;

- Raman light scattering measurements were performed in cooperation with the Department of Physics and School of Nano Convergence Technology at Hallym University Chuncheon, Korea. The measurements were carried out in a micro-backscattering system using a 532 nm wavelength laser and a conventional Raman spectrometer (LabRam HR800, Horiba, Co., Kyoto, Japan) combined with a temperature adapter (THMS600, Linkam, Surrey, UK). Olympus BX41 optical microscope was used for this geometry. The Raman spectrum was measured to approximately 10 cm^{-1} using a holographic cut-off filter. A single diffraction grating with the density of 1800 lines/mm was used, resulting in the resolution of 0.5 cm^{-1};

- conventional Fabry–Perot coupled interferometer was used to measure the Brillouin scattering spectrum in the range of ±60 GHz. The sample was placed in Linkam THMS 600 temperature adapter; BX41 manual Olympus microscope was used to measure scattering in backscattering geometry. Solid-state laser (Excelsior 532–300, Spectra Physics, Santa Clara, CA, USA) with a wavelength of 532 nm was used as the excitation source. Details of the spectrometer used in the study can be found in [57]. Brillouin scattering studies were performed in collaboration with the Department of Physics and School of Nano Convergence Technology at Hallym University Chuncheon, Korea;

- electron structure studies were performed using X-ray photoelectron spectroscopy (XPS), using Physical Electronics PHI 5700/660 spectrometer with monochromatic Al K_α radiation (1486.6 eV). An electron gun was used to compensate for the charge generated on the surface during irradiation of the sample. A detailed description of the data analysis is presented in [31];

- the analysis of ion distribution in $PbZrO_3$ crystals, in the form of depth profiles, was carried out using IONTOFToF-SIMS V spectrometer, a high-energy beam that emits secondary ions (and ion clusters from the surface of the sample), and a low-energy etching beam that operated in double-beam mode. The analysis was carried out using a single isotope ion beam emitted in the form of high-energy pulses (Bi^+ ion beam with 30keV energy, with target current of approximately 1.4 pA). Digestion was carried out using high current, but with lower source energy (Cs beam operating at 1 kV and 50 nA). This beam etched a $600 \times 600 \text{ μm}^2$ crater, while the bismuth ion beam gradually analyzed the crater bottom. Due to the need to eliminate the effects associated with the heterogeneity of emissions at the edges of the crater, the analysis area has been narrowed down to $167 \times 167 \text{ μm}^2$. The details of the analysis and the experiment are described in [31];

- structural tests were carried out using the powder method, by means of PANalytical PW1050 diffractometer using a nickel filter and $CuK\alpha_{1.2}$ X-ray source operating at 30 kV/30 mA. Structure refinement was carried out using the Rietveld method [58], applying FULLPROF software [59]. The details of individual experiments are presented in [32,33,38];

- crystals of $PbZrO_3$ doped niobium were characterized for chemical composition by using energy-dispersive X-ray fluorescence spectrometer (EDXRF), epsilon 3 (Panalytical, Almelo, The Netherlands) with mercury pipe as the X-ray source at the maximum voltage of 30 keV and 9 W. The spectrometer was equipped with a thermoelectrically cooled silicon drift detector (SDD) with 8mm beryllium window and the resolution of 135 eV at 5.9 keV. Quantitative analysis was performed using Omnian software. Details of the measurements are presented in [33];

- chemical analysis of pure $PbZrO_3$ crystals and Bi_2O_3 doped PZT 70/30 ceramics was performed using JSM-5410 scanning electron microscope from Jeol, equipped with energy-dispersive X-ray spectrometer (EDS) from Oxford Instruments.

3. Results and Discussion

The summary can be divided into four main sections: **1.** The effect of defects on phase transitions in pure $PbZrO_3$ crystals [31]. **2.** The effect of an admixture of niobium on compensation or creation of

defects in the PbZrO$_3$ crystal lattice, and the impact of these phenomena on local breaking of symmetry above T$_c$, connected with instability of crystal lattice vibrations [32–36]. Special attention should be paid to the fact that these studies were used in a variety of research techniques, allowing researchers to look at the problem from the point of view of local structure changes and macroscopic properties of the tested materials. The self-organization of a crystal structure at a constant temperature, not known well as yet, will also be presented [36]. **3.** The third problem considered is the segregation of defects caused by the action of an alternating electric field [37]. This issue is particularly important in the context of potential applications of the tested materials. **4.** The fourth issue raised in [38] is the impact of lead sublattice defects on polar regions, occurring above T$_c$ in PZT 70/30 ceramics doped with Bi. The relationship between polar regions and instability of vibrations in the crystal lattice of the examined materials is discussed.

Therefore, this summary aims demonstrate—based on pure and doped antiferroelectric PbZrO$_3$, and materials synthesized as based on it—an influence (a role) of defects on crystal lattice instabilities which de facto decide on type of transitions which these materials undergo, and on local symmetry breaking phenomenon that start appearing in ABO$_3$ perovskites already far above T$_c$.

3.1. Induction of the Intermediate Phase by Means of Crystal Lattice Defects in PbZrO$_3$ Single Crystals [31]

Calculations of the total energy of lead zirconate structure show that there is instability in terms of antiferroelectric and ferroelectric distortion of lattice, indicating a delicate balance between them [60–62]. Therefore, we deal with a state of unstable equilibrium, where an additional factor, such as network of defects or weak electric field, can induce the ferroelectric phase inside the antiferroelectric phase in PZO ceramics [63]. Recent studies of lattice dynamics showed that the intermediate phase is a result of coexistence of the antiferroelectric and paraelectric phases below T$_c$ [29]. This fact is related to the occurrence of lattice instability above T$_c$, causing the existence of polar regions, as mentioned in the introduction. As stated in [64], these regions occur due to disorder in the lead sublattice above T$_c$. This disorder results from the hybridization of lead electrons and oxygen p electrons in the paraelectric phase [65]. It could therefore be concluded that defects both in the oxygen and lead sublattice affect only the lattice instability in PbZrO$_3$ and polar fluctuations above T$_c$. In the literature, however, the role of zirconium and defects in the zirconium sublattice is completely ignored, considering this sublattice as stable and with no impact on those instabilities. However, looking at the basic order parameter of the phase transition in PbZrO$_3$, which is associated with the anti-parallel arrangement of pairs of lead atoms and tilts of ZrO$_6$ octahedra, both conditions may lead to the appearance of antiferroelectricity in this material [24]. Therefore, the role of zirconium and the presence of defects in the zirconium sublattice should not be overlooked in the consideration of phase transitions that PbZrO$_3$ undergoes.

With a PbZrO$_3$ crystal in which there is no intermediate phase, one can prove that defects are responsible for the occurrence of intermediate phase [31]. It is enough to deliberately produce crystal defects in a controlled manner, e.g., in high vacuum conditions in specified time, and at a certain high temperature [31]. Observations of the birefringence maps in a virgin crystal, in which no intermediate phase was observed, and then in the same crystal defected in a vacuum, showed a dependence of the width of temperature range, in which an intermediate phase could be observed, with the concentration of lattice defects. It was directly related to the annealing temperature T$_H$ of crystal in a vacuum (Figure 1).

Figure 1 shows that dependence of transition temperature on annealing temperature, i.e., on the concentration of defects, is not a monotonic function. Systematic studies of both the distribution of elements within the sample, their mutual concentration and oxidation states, could create a coherent picture of defect chemistry in PbZrO$_3$ and thus their impact on transition phase.

Tests using the TOF-SIMS method showed a substantial chemical heterogeneity of virgin crystal to the depth of approximately 35–40 nm in all sublattices (Figure 2).
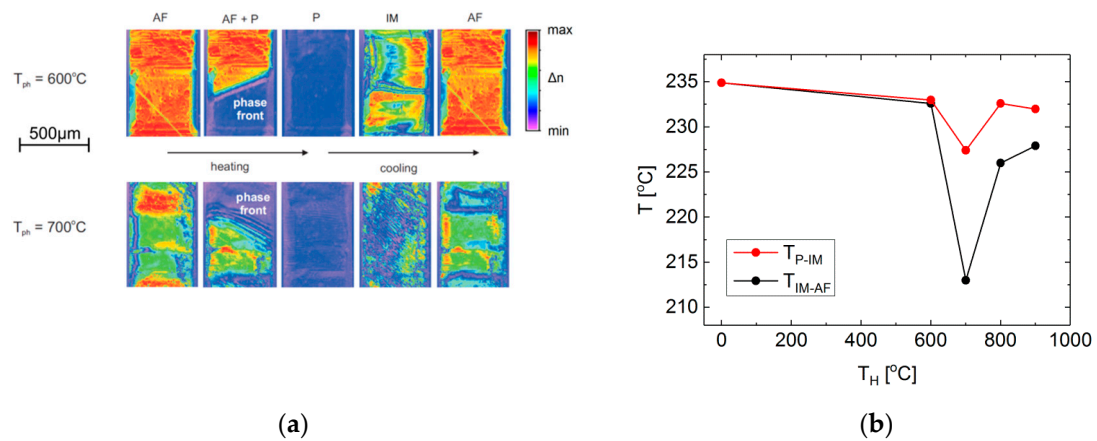
(a) **(b)**

Figure 1. (**a**) Maps of birefringence obtained on heating and cooling. The color change from pink to red (as seen in the phase front of the transition from antiferroelectric (AF) to paraelectric (P) phase) indicates the changes in birefringence from minimum to maximum value. The phase transition from AF to P state could be observed on heating, and from P state to intermediate phase (IM) on cooling. Along with further reduction of temperature, it was possible to observe the transition from IM to AF phase; (**b**) Phase transition temperatures from P to IM (denoted as T_{P-IM}) and from IM to AF phase (denoted as T_{IM-AF}) as a function of annealing temperature T_H, obtained on cooling [31].
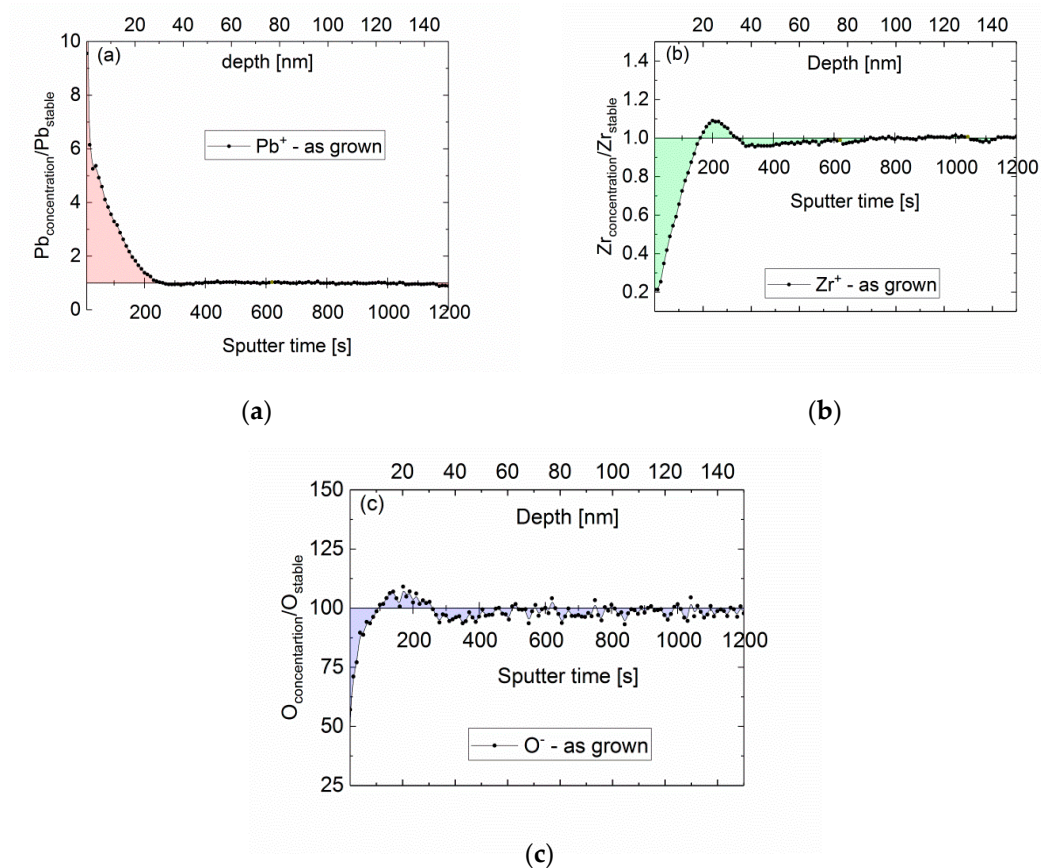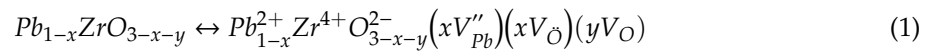

(a) **(b)**

(c)

Figure 2. Depth profiles obtained by the TOF-SIMS method for (**a**) lead, (**b**) zirconium and (**c**) oxygen in virgin PbZrO$_3$ crystal [31] (index "stable" means the stable concentration of the element in the crystal interior).

The absence of a phase transition in such crystal may be due to the presence of an external factor, such as chemical pressure produced by non-stoichiometric crystal surface layer. When the crystal is

annealed at relatively low temperatures (500, 600 °C), the amount of lead released from the surface layer decreases and the crystal can be considered to be a compensated semiconductor governed by the equation:

$$Pb_{1-x}ZrO_{3-x-y} \leftrightarrow Pb_{1-x}^{2+}Zr^{4+}O_{3-x-y}^{2-}\left(xV_{Pb}''\right)\left(xV_{\ddot{O}}\right)\left(yV_{O}\right) \tag{1}$$

where V_{Pb}'', $V_{\ddot{O}}$ and V_{O} stand for the lead vacancy with a double positive charge, oxygen vacancy with a double negative charge and electrically neutral oxygen vacancy, respectively.

Research of the electronic structure allowed the determination of degree of oxidation for individual elements, in particular lead and zirconium (Figure 3).
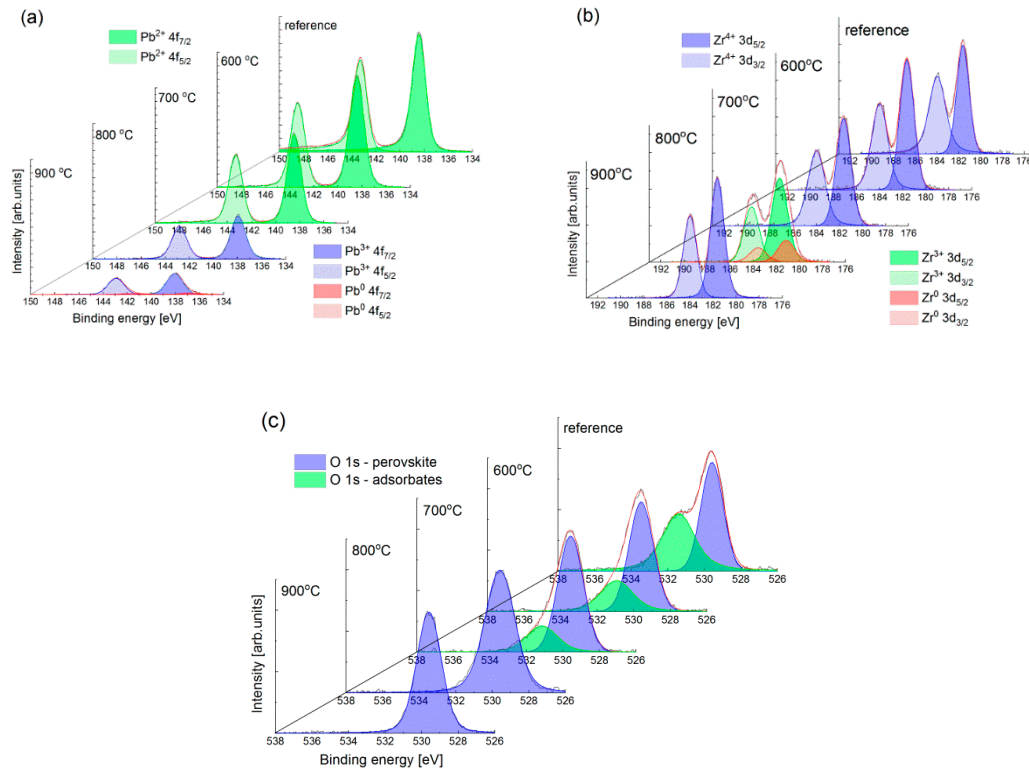

Figure 3. Core electron states of (**a**) lead 4f, (**b**) zirconium 3d, and (**c**) oxygen 1s for a virgin sample and sample after annealing at 600, 700, 800 and 900 °C [31].

Knowing the relative changes in the concentration of individual ions, it was possible to determine the chemistry of defects for specific characteristic ranges of soaking temperatures. Thus, for temperature T_H in the range between 600 and 700 °C, the crystal can be considered to be a compensated n-type semiconductor, wherein an important role is performed by double-ionized oxygen vacancies and ionized zirconium vacancies. These defects can be trapping centers for holes or electrons, which can be filled on cooling and emptied on heating. For the annealing temperature of 700 °C, the concentration of these traps results in a significant extension of the temperature range in which the intermediate phase appears. On microscopic scale, in some parts of the crystal volume these traps become full, and at the same time remain empty in other parts. Based on recent Brillouin light scattering, which shows that transition phase is the coexistence of the paraelectric and antiferroelectric phases [29], it can be concluded that the existence and states of filling of these traps are responsible for the phase transitions. It means that filled traps help the occurrence of antiferroelectric phase, and vacant traps help the occurrence of paraelectric phase. One can simply say, as presented on heating [31], that the trap centers are systematically emptied, and all are empty at a certain temperature. On cooling, these centers are filled up again. Depending on the energy levels of the trap centers, their "empty" or "full" state depends on temperature. Therefore, in the lead or zirconium sublattice, some centers may become full

and some may remain empty. These centers (and in fact their effective charges) affect the vibrations of crystal lattice, thus the occurrence of two states of trap centers can strengthen the coexistence of phases in connection with interrelation between optical and acoustic vibrations. To some extent, the existence of such defects may affect the stabilization of "precursors" at temperatures higher than T_{BH} known from theoretical model ($T_{BH} = 1.1\ T_c$).

As can be seen in Figure 4, further increase of defects concentration in $PbZrO_3$ leads to changes in the valence of lead from Pb^{2+} to Pb^{3+}, and at 900 °C metallic lead can also be observed. In the case of zirconium, metallic state appears at 800 °C, and after further heat treatment it is re-oxidized by oxygen ions from the inside of the crystal. At the same time, a drastic reduction of the temperature range is noticed, in which the intermediate phase occurs. This means that these types of defects negatively affect the coexistence of phases, favoring the antiferroelectric phase. In [31], an in-depth analysis of such cases was also carried out in terms of defect chemistry.
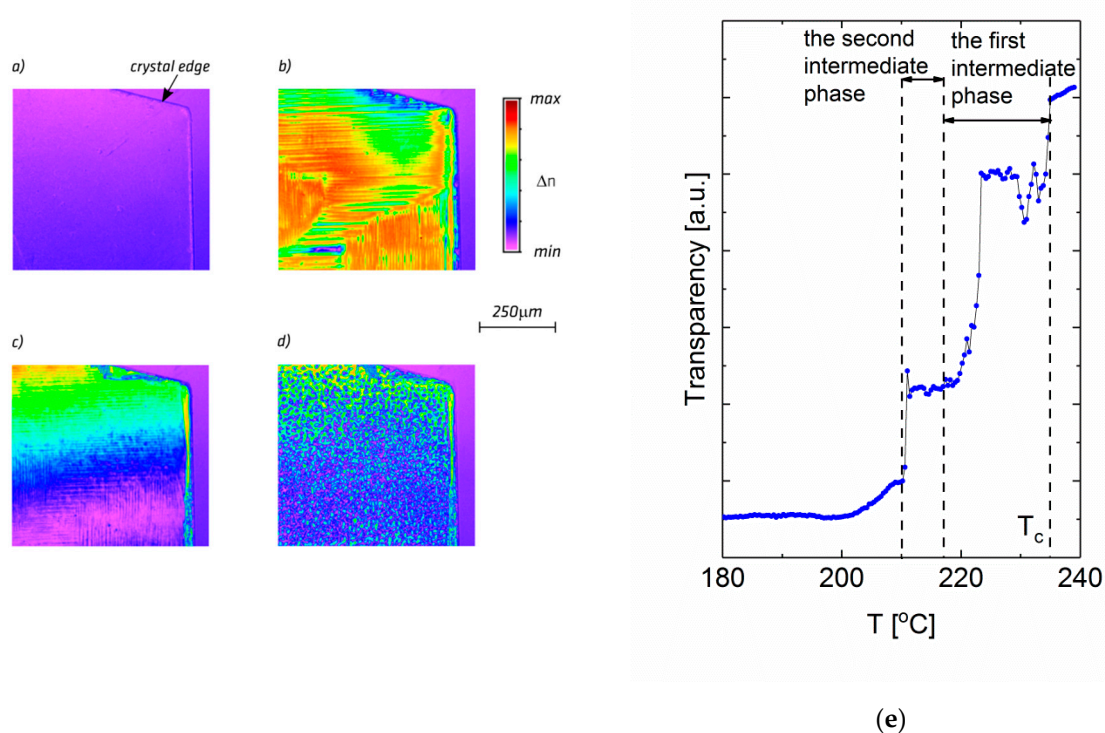

(e)

Figure 4. Birefringence maps of $PbZrO_3$ single crystals with the nominal content of 0.6 mol% Nb_2O_5 obtained in the cooling process (**a**) above T_c at 235 °C, (**b**) below T_c in the first transition phase, at 229 °C, (**c**) in the second transition phase, at 215 °C, and (**d**) in the antiferroelectric phase, at 186 °C. The bar with a color gradient represents birefringence values from 0 (pink) to the highest value (red) [32]. The Figure 4**e** shows the dependence of light absorption at 570 nm wavelength in $PbZrO_3$ with an admixture of nominal amount of 1 mol% Nb_2O_5 as a function of temperature in the cooling process, for wavelength $\lambda = 570$ nm [33].

The following facts should be considered now:

- the occurrence of transition phase depends on the ratio of donor and acceptor centers. Because this ratio is not in equilibrium, full or empty centers act as a local stress fields, thus locally affecting lattice vibrations and the occurrence of intermediate phase, disturbing the delicate energy balance mentioned above;
- defects in the zirconium sublattice should also be taken into account as being responsible for the existence of intermediate phase;

- all occurring centers, being in different states of filling/ionization, strengthen the possibility of phase coexistence. Thus, it was found that the occurrence of these centers is the main cause of local symmetry violation, which plays an important role in the occurrence of intermediate phase in $PbZrO_3$.

3.2. Influence of Donor Dopant in the form of Niobium Atoms on the Dynamics of the PbZrO$_3$ Crystal Lattice and Local Symmetry Breaking Above T$_c$ [32–36]

The introduction of admixtures with similar ionic radii in relation to the ionic radius of ions replaced in the lattice, but with different valence will lead to the creation or compensation of network defects. Compensation or creation of defects will take place depending on the ratio of the amount of dopant to *natural* defects, which occur during the production of the material. In the case of lead zirconate, defects arising during growth are discussed in [31]. The articles [32–36] directly show the effect of a hetero-valent dopant, which was niobium atoms, on both breaking of local symmetry and phase transitions observed in the tested materials.

The first important fact is the observation of a new phase transition for samples with different dopant concentrations [32,33] and for crystals obtained in other growth process [34]. Regardless dopant concentration or growth process, the additional phase transition, previously not observed in $PbZrO_3$ ceramics doped with niobium, was observed by means of various research techniques: observation of domain structures and birefringence [32–34], dielectric tests [32–34], electromechanical tests [32,33], Raman [34] and Brillouin [35] light scattering.

Domain structure studies using birefringence maps or a polarizing microscope have clearly demonstrated the existence of different domain structures indicating the existence of new phase transition (Figure 4)

In addition, the so-called post-transitional effects (Figure 4e) in the temperature range from about 210 °C to 200 °C, in which the coexistence of second phase transition (IM2) and antiferroelectric phase (AF) was postulated.

Studies of the piezoelectric phenomenon have shown that both intermediate phases are polar under the influence of the applied electric field [32,33]. Piezoelectric effect above T_c has also been found. This fact was confirmed by birefringence studies of crystals (Δn) (Figure 5), showing that local symmetry violations can occur even at temperatures higher than those at which piezoelectric effect appears. This difference results directly from the greater sensitivity of the method of birefringence measurements [33]. The temperature range in which non-zero birefringence exists is broadened with increasing dopant concentration [32,33], including temperatures higher than $T_{BH} = 1.1\ T_c$ (in Kelvins) for higher dopant concentrations [33,34]. This fact is directly related to the types of defects described in [32]. Specifically, the admixture of niobium—due to its ionic radius—most likely takes replaces zirconium in the crystal lattice. Therefore, 4 scenarios are possible:

(1)　niobium changes its oxidation state to 4+ giving one electron to the conductivity band,
(2)　niobium is situated next to lead vacancy, which means that two niobium atoms can compensate for the double-ionized lead vacancy,
(3)　two niobium atoms generate one compensated lead vacancy.
(4)　one should take into account the possibility of contaminants in the used culture substrates, such as sodium or potassium, which are ionized to generate oxygen vacancies. In this case, two niobium atoms will compensate for a double-ionized oxygen vacancy.

As in pure lead zirconate, in doped crystal the atom in the middle of oxygen octahedrons is responsible for the stabilization of intermediate phase, and even for the generation of a new, not observed as yet, second transition phase.

In the case of a crystal with nominal niobium content of 0.6 mol% Nb_2O_5, the temperature of birefringence and piezodeformation decay (T_{BH}) is consistent with theoretical predictions; the T_{BH} for this material is about 280 °C [32]. On the other hand, for crystals with admixture concentration

of 1 mol%, the temperature of birefringence decay is distinctly higher than T_{BH} and equal to 285 °C. This fact can be easily explained by the fact that in the first case niobium led to compensation of the charge of lead vacancies, while in the second case niobium led to the creation of new defects, by which the local symmetry breaking has taken place at temperatures above T_{BH} [33].
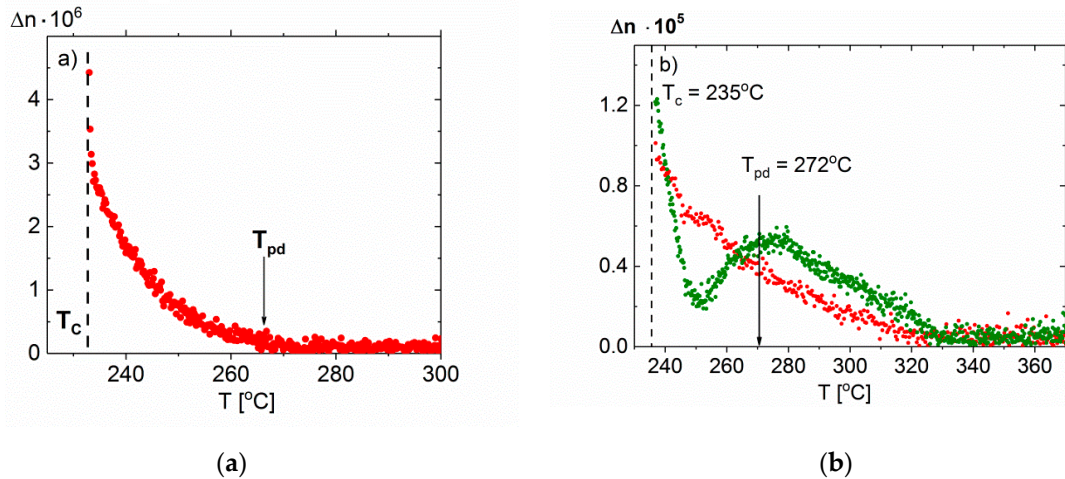

Figure 5. Birefringence above T_c for PbZrO$_3$ crystal doped with (**a**) 0.6 mol% Nb$_2$O$_5$ [32] and (**b**) 1.0 mol% Nb$_2$O$_5$ [33]. T_{pd} is the temperature at which the piezo-deformation signal disappears.

The presence of an additional phase transition prompted us to try to obtain crystals from other chemical substrates, excluding PbZrO$_3$ ceramics doped with Nb$_2$O$_5$. The results were crystals used in investigations reported in [34,35]. They also showed an additional phase transition both in observations of the domain structures using a polarizing microscope and in dielectric studies [34], which proves that intermediate phase is appropriate for this group of materials. Also, in these materials the so-called pre- and post-transition effects occur, i.e., breaking of local symmetry above T_c, and below the transition from the second intermediate phase to AF state [34].

To understand better the nature of those two intermediate phases and to answer the question concerning the exact reason for local symmetry breaking above T_c, investigations in microscale of Raman [34] and Brillouin light scattering [35] were performed.

The study of Raman scattering revealed the first order Raman spectrum above T_c, which would not be possible if the paraelectric phase was centrosymmetric [66]. These studies confirm local violation of symmetry above T_c in niobium-doped PbZrO$_3$ crystals [34]. The Raman spectra obtained (Figure 6a) were fitted with a function containing a set of suppressed harmonic oscillators (Equation (2)), where: S_i, ω_i, γ_i are the oscillator strength, the frequency and the damping factor of i-th phonon mode, respectively. S_r and γ_r denote the strength and relaxation rate of a relaxor, respectively. The terms $(n(\omega)+1)$ and $n(\omega)$ are the Bose–Einstein factors that correspond to the Stokes and anti-Stokes scattering. It allowed determining the frequency of individual vibrations of the crystal lattice (Figure 6b,c) [34]. Because the investigated crystals were in multi-domain state, direct indexation of the modes was impossible. However, due to small light spot used it was possible to observe the partly polarized Raman modes, although crystallographic orientation of the domain was not known.

$$I_R(\omega) = \left\{ \begin{array}{c} n(\omega) + 1 \\ n(\omega) \end{array} \right\} \left(\frac{S_r \gamma_r \omega}{\omega^2 + \gamma_r^2} + \sum_i \frac{S_i \omega_i^2 \gamma_i \omega}{\left(\omega_i^2 - \omega^2\right)^2 + \gamma_i^2 \omega^2} \right) \qquad (2)$$
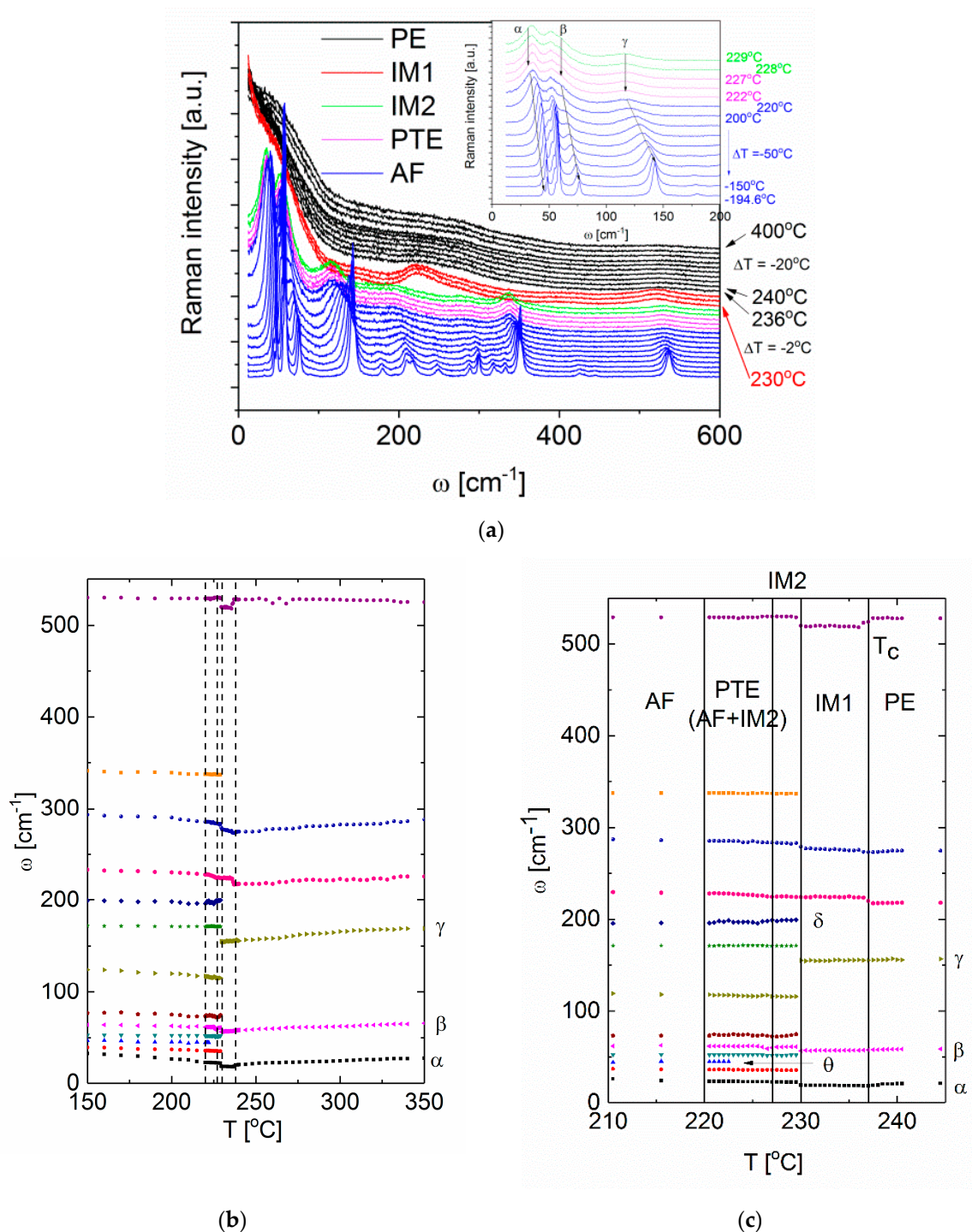
(**a**)

(**b**)　　　　　　　　　　　　　　(**c**)

Figure 6. Temperature (**a**) evolution of Raman spectra and (**b**) dependence of lattice vibration frequency for the PbZrO$_3$:1%Nb crystal. Dashed lines correspond to the temperatures of phase transitions determined from dielectric and optical studies [34]; (**c**) temperature lattice vibration frequency in vicinity of phase transitions for the PbZrO$_3$:1%Nb crystal.

It was found that on cooling, after exceeding T$_c$ the number of modes does not change, which may suggest that polar regions in the paraelectric phase determine the structure of the first intermediate phase. Because the Raman spectra of the first intermediate phase resemble the spectra of Pb(Zr,Ti)O$_3$ with low titanium content, it can be assumed that this phase has a rhombohedral structure. Only the transition to the second intermediate phase causes an increase in the number of lattice vibrations

(Figure 6b,c). In the temperature range at which transient effects were noted, the coexistence of a second intermediate phase and antiferroelectric phase was demonstrated, the appearance of which was noted by the appearance of a mode marked θ (Figure 6c). This mode occurred at temperature below the temperature range, in which intermediate effects occur [34].

Among the matched modes, the occurrence of three softening modes shown in Figure 6a and c as α, β and γ was found, which confirms the tests carried out for pure $PbZrO_3$ [67], in which softening at least of several branches of the crystal lattice modes is responsible for phase transition in $PbZrO_3$. However, after careful analysis, it turns out that only α vibration softens when approaching T_c and hardens below it. After plotting the $\omega^2(T)$ dependence for these three modes, which according to Cochran's law should be a linear function of temperature, it turned out that two of them, i.e., β and γ, do not satisfy this law in a certain temperature ranges (Figure 7).
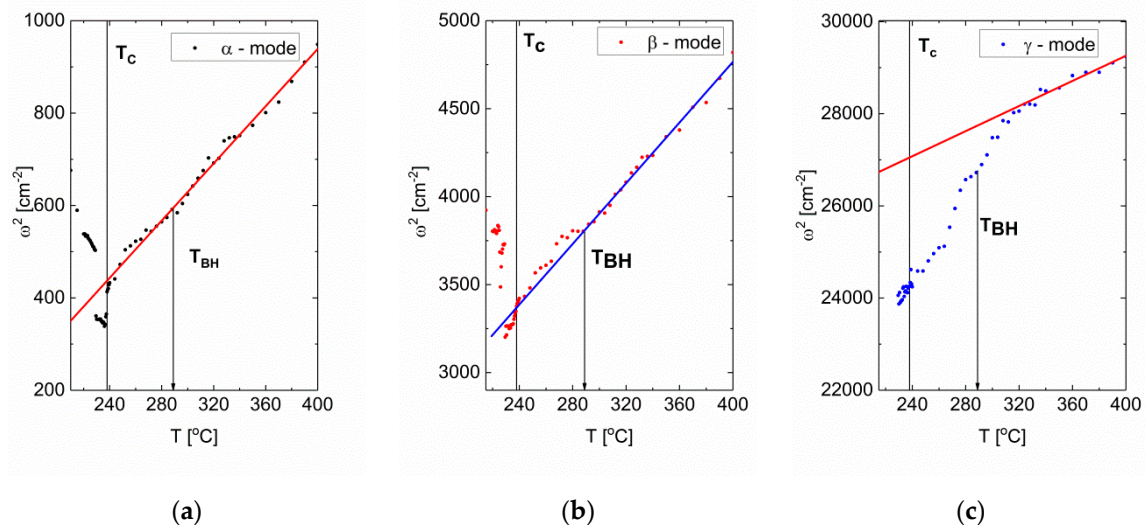

Figure 7. Temperature dependence of the squares of modes' frequencies (**a**) α, (**b**) β and (**c**) γ. The red and blue lines match in high temperature range. The temperature defined in [34] was determined as T_{BH}.

Thanks to papers [68,69] it was possible to determine which atoms these three modes are related to. The α mode is associated with the vibrations of lead ions. Its observation above T_c must be related to structural disorder in this sublattice, causing local symmetry breaking. However, as one can see, it is not subject to any anomaly in T_{BH}. This disorder is, however, responsible for phase transition to macroscopically polar phase, which is the first intermediate phase (IM1). The β mode can also be attributed to the vibration associated with lead atoms. As can be seen, this mode experiences a noticeable anomaly in T_{BH}, which complies with theoretical assumptions [30]. It can therefore be concluded that the admixture of niobium does not affect this type of local symmetry violation, because it concerns directly sublattice A, but not B, in which—as was assumed—niobium is present. The oscillation of γ mode should point to oxygen octahedra vibration as being responsible for their tilts. Thus, it can be seen that the admixture of niobium affects the vibrations of oxygen octahedrons, which leads to breaking the symmetry well above the limit set by temperature T_{BH}. This confirms the earlier conclusions from studies [32,33] that the admixture of niobium stabilizes the local symmetry breaking above T_c and is placed inside the BO_6 octahedron. Also, due to the greatest discontinuity of changes in the γ frequency at transition temperature between the IM1 and IM2 phases, it can be stated that the admixture of niobium is responsible for the occurrence of this phase transition and the appearance of a new intermediate phase, not observed as yet (IM2). The phase transition itself should be realized mainly by a change in the tilts of oxygen octahedra.

Paper [34] is a report concerning observations of the quasi-elastic light scattering that contains the so-called central peak. This suggests that phase transitions observed can be caused either by

a relaxation process existing above T_c or by some kind of disorder in sublattices, being of static or dynamic character. The reason for that may be clustering of niobium-containing cells in the crystal lattice, which would confirm the assumptions made in [32] in connection with the observed birefringent circular regions of micro-meter size in the antiferroelectric phase. It is worth mentioning that niobium clustering process was observed in $SrTiO_3$ just doped with niobium [70].

As continuation of the studies of crystal lattice dynamics, Brillouin light scattering studies were performed [36] in the backscattering geometry. Only longitudinal acoustic mode (LA) was observed, which on cooling there was a split at 227 °C, i.e., at the temperature at which post-transitional effects occur. These two modes were coexisting up to 200 °C (Figure 8) which would mean that coexistence of phases occur in a much wider temperature range than previously found [35]. Therefore, it points to the phase transition nature different from that in pure $PbZrO_3$, in which the antiferroelectric and paraelectric phases coexisted in the intermediate phase [29].
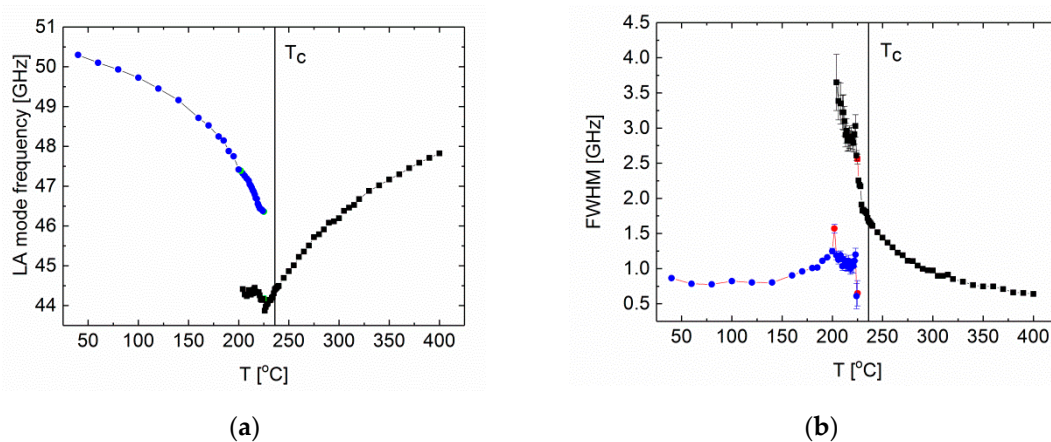

Figure 8. Temperature dependence of (**a**) the LA mode frequency shift and (**b**) the half-width of this mode, determined from the Brillouin light scattering [35].

Unexpectedly, the LA mode frequency and half-width appear to be insensitive to phase transition at T_c and at transition between IM1 and IM2 phases. The derivative of half-width versus temperature shows an increase of the speed of mode damping at temperature about 320 °C. This temperature is associated with the appearance of polar regions observed in the Raman light scattering [34] and corresponds very well to the mode describing tilts of oxygen octahedra mentioned above. Therefore, it is another proof that in the paraelectric phase local polarity is induced due to an interaction between acoustic and optical modes (lattice instability), as suggested in theoretical model by Bussmann-Holder in [30].

Due to large temperature hysteresis of properties observed for niobium-doped crystals in the IM1 and IM2 phases on cooling and heating, one can suspect that it stems from a metastable process [32–34]. In [35], the stability of IM1 phase in time was controlled through measurements of the dielectric, optical, and pyroelectric properties at constant temperature and over time. That was carried out on cooling when the width of temperature range of the IM1 phase is greater than on heating. Examples of time changes of the permittivity are shown in Figure 9.

These experiments show that while temperature is stabilized at 217 °C, a phase transition from the phase IM1 to IM2 takes place spontaneously after a defined time. The same results were obtained by measuring the pyroelectric current. After approximately 21 min, changes in the current flowing in the system maintained at constant temperature were of the same character as those observed later during IM1 to IM2 transition on cooling. It means that we must deal with isothermal phase transition, at which at constant temperature a part of the sample transforms to the IM2 phase. This kind of transition was observed for all investigated samples, i.e., samples with different Nb concentrations, and for samples obtained in different technological processes. This proves that we deal with a process

of self-organization of crystal lattice at a constant temperature, which is appropriate for lead zirconate crystals doped with Nb and has long-term relaxation character.
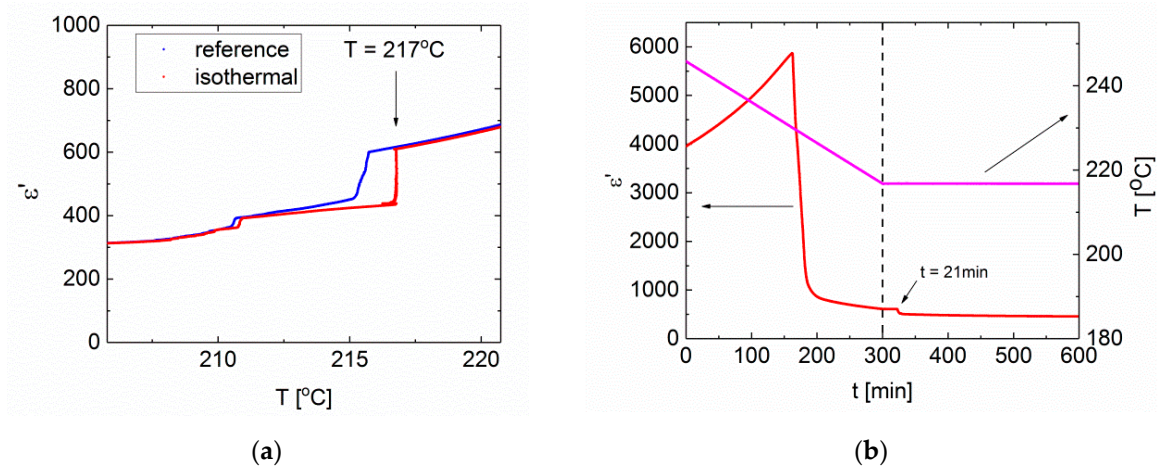

Figure 9. (**a**) Dielectric changes for the reference $\varepsilon(T)$ run (blue curve) and $\varepsilon(T)$ run (red) after keeping the sample at 217 °C for 21 min (red); (**b**) Changes of permittivity (red) and temperature (pink) as a function of time [36].

The most important conclusions from the experiments presented above, described tentatively in [32–36] papers, include:

- discovery of new, previously unobserved, phase transition and characterization of the nature of two intermediate phases,
- determination of the role of central ion in oxygen octahedron in polar regions, occurring above T_c,
- experimental confirmation of a specific interrelation (coupling) between acoustic, and optical modes of crystal lattice above T_c,
- demonstration of coexistence of intermediate phase (IM2) and antiferroelectric phase (AF), and the relaxing nature of phase transition between IM2 and IM1 phases.

3.3. Segregation of Lattice Defects in PbZrO₃ Crystal Doped with Niobium by Alternating Electric Field [37]

In the investigation of dielectric and electromechanical properties of perovskites containing oxygen octahedra, well known as functional materials, alternating or constant electric fields are used. However, the effect of these fields on surface properties is not taken into account sufficiently. For this reason, studies have been undertaken on the impact of alternating electric field on phase transitions and chemical properties of niobium-doped $PbZrO_3$ crystals surface. That is why crystals, in which the concentration of admixture was high enough to create defects in the crystal lattice, have been investigated [37].

It has been found that alternating electric field changes the share of crystal part directly under the electrodes (surface) and its interior in the dielectric response. Study [37] has shown for the first time how important it is and what misleading conclusions may be drawn without that knowledge of phenomena presented in that paper. What is unique about that research is that measurements were performed on two parts of the same crystal, while only one was connected to an electrode (part B in Figure 10). Hence, only one part of the crystal was subjected to an electric field. It was, however, obvious that both parts of the crystal had the same "history" from the point of view of temperature changes it was subjected to.
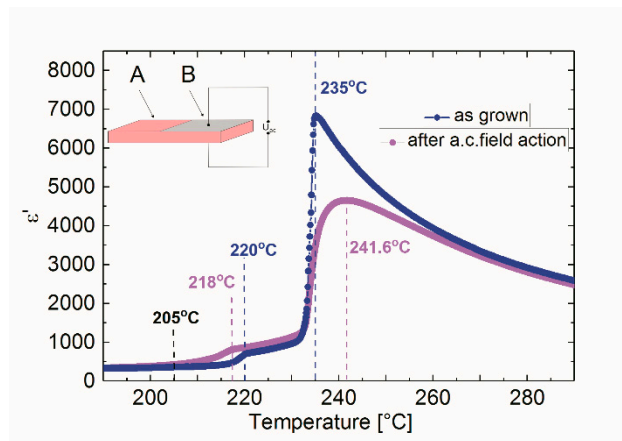
Figure 10. Temperature changes of electric permittivity of the virgin crystal part A (blue) and part B of crystal exposed to alternating electric field (magenta). The inset shows the geometry of electrodes used for dielectric and electromechanical measurements. The measuring field frequency in dielectric measurements was 1 MHz and the electric field strength in electromechanical measurements was 3 kV/cm [37].

As Figure 10 shows, the action of alternating electric field increases the temperature at which the maximum of $\varepsilon(T)$ run, pointing to T_c, takes place, and decreases the transition temperature between IM1 and IM2 phases. However, temperature changes of the sample clearly demonstrate that linking the maximum of the $\varepsilon(T)$ run with T_c is incorrect. Due to internal friction during sample vibrations in alternating field, heat is generated in the sample, which can be determined by measurement the deformation and temperature of the sample simultaneously. An example of such measurement is shown in Figure 11.
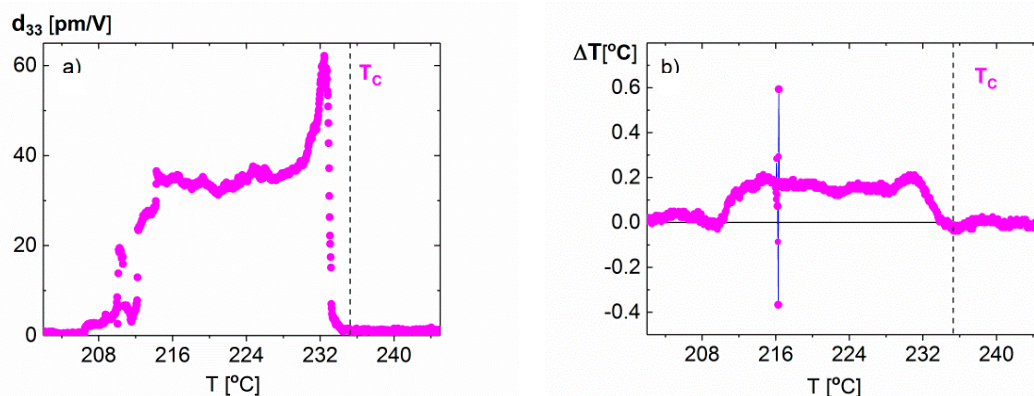

Figure 11. (**a**) Temperature changes of d_{33} piezoelectric module and (**b**) changes of sample temperature caused by phase transition enthalpy and/or internal friction caused by movements of domain/polar regions under the influence of an external alternating electric field. The measurement was made on cooling [37].

The observed temperature changes (Figure 11) clearly indicate that temperatures of phase transitions have not changed. Therefore, a question is raised why different runs of permittivity as function of temperature have been observed. The answer is that there is a change of physical properties mainly in crystal surface after application of a.c. field. The use of XPS techniques has shown that as a result of this action, the crystal surface is oxidized and lead appears in the fourth degree of oxidation, observed only inside the virgin part of the crystal. Moreover, valence band studies have shown the expansion of energy gap after electric field action in relation to the energy gap inside the virgin crystal [37]. This means that from the inside of the crystal, the defects were transported towards

the surface, improving the quality of the interior and changing the chemical properties of surface. Thus, dielectric response measured after a.c. field action is a kind of "averaged" response from the surface–interior–surface system.

The most important conclusions are the following ones:

- there is a complex relation between the interior and surface of a crystal subjected to a strong alternating field that may cause misleading interpretation of the dielectric response,
- a possibility exists of "cleaning" the interior of the crystal by transporting defects towards the surface, enabled by alternating electric fields.

3.4. Interactions between Polar Regions Occurring Above T_c in $PbZr_{0.70}Ti_{0.30}O_3$ Ceramics Doped with Bismuth [38]

Lead zirconate titanate (PZT) with higher content of titanium than zirconium and with different admixtures is widely used in applications. The paper [38] shows the influence of bismuth on physical properties of PZT 70/30 ceramics. It shows that increase in the concentration of bismuth reduces the temperature of phase transition from paraelectric to ferroelectric phase and reduces dielectric dispersion. This is probably due to the occurrence of four scenarios, whose probability varies with the amount of dopant concentration [38]. Namely:

(1) two Bi^{3+} ions compensate for a double-ionized lead vacancy formed in the process of synthesis,
(2) two Bi^{3+} ions produce one lead vacancy,
(3) one ion of Bi^{3+} compensates for Ti^{3+} ion, which may occur due to the existence of oxygen vacancies [71],
(4) Bi^{3+} ion leads to a change in oxidation state of ion in the middle of oxygen octahedron from 4+ to 3+. The most likely reason for it is a change in the valence of titanium due to its lower chemical stability than that of zirconium; such effects have also been observed in PZT 70/30 ceramics doped with $BiMnO_3$ [72].

However, the most important fact presented in [38] is the interaction between polar regions. They were observed by measuring birefringence and dielectric properties of PZT doped with Bi (Figures 12 and 13) [38].
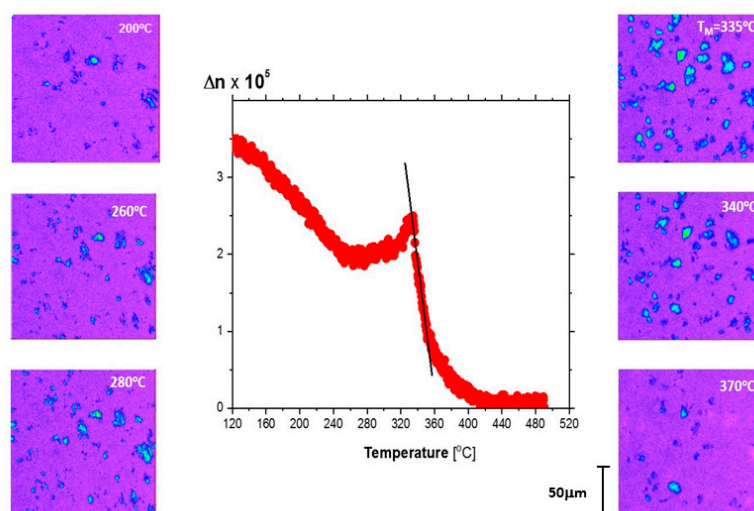

Figure 12. (middle part) Temperature changes of birefringence (average values), after subtracting the background generated by the set-up, for areas of $500 \times 450 \ \mu m^2$ of ceramics PZT70/30 doped with 0.2 mol% Bi_2O_3. This area contains over 200 grains. On the left and right side there are birefringence maps for selected temperatures, showing the evolution of polar regions in terms of size. The size of birefringent regions (blue bright spots) is interpreted as size of polar regions. Linear changes of Δn as function of temperature were observed above the T_m temperature (maximum of permittivity) [38].
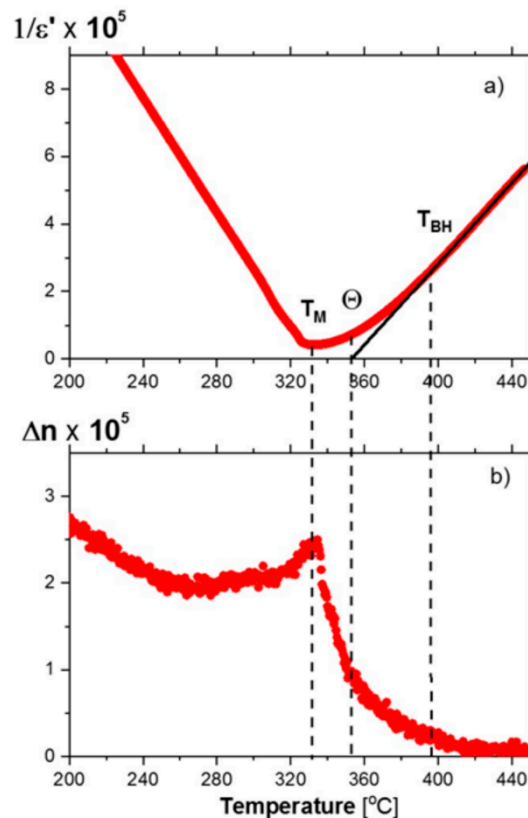
Figure 13. Changes in the inverse of permittivity and birefringence (average value) as a function of temperature for PZT 70/30 ceramics doped with 0.2 mol% Bi_2O_3, obtained on heating. (**a**) Inverse permittivity showing temperature T_M, Curie–Weiss temperature θ, as determined from $\varepsilon^{-1}(T)$ run, and temperature T_{BH} calculated from the formula $T_{BH} = 1.1\,T_M$; (**b**) temperature changes of birefringence determined from the area of 500×450 μm^2 of ceramics with 65 μm thickness [38].

As can be seen from Figure 13, the polar regions increase in size up to the temperature at which the maximum of permittivity occurs. The comparison of average changes of birefringence with changes of inverse permittivity gives very interesting correlation and explains the fact that temperature θ, which in the Curie–Weiss law should be less than or equal to T_M, is apparently higher than T_M (Figure 13).

As can be seen from Figure 13, the Curie–Weiss law is not obeyed below T_{BH}, which is in line with theoretical predictions [30] However, this fact was observed only for the lowest concentration of Bi, and with further increase in concentration, the temperature at which deviation from the Curie–Weiss law was observed was higher than T_{BH}. This fact can be explained by creating defects in the lead sublattice, as was case of Nb-doped crystals, or by changing the valence of the cation located in the middle of oxygen octahedron, i.e., titanium which changes its valence to Ti^{3+}. This additional defect produces local stress that stabilizes the occurrence of polar regions at higher temperatures.

Further analysis of Figure 13 allows the drawing of a conclusion that the maximum of permittivity appears as a result of increased sizes of polar regions, and thus their long-range interactions. Therefore, the maximum of permittivity does not have to be associated with any structural phase transition. As can be seen, above temperature T_M, the material is not in paraelectric phase in its entire volume, due to the presence of polar regions at least up to T_{BH}.

However, how to interpret temperature θ remains to be explained. Based on the results presented in Figure 13, it may be assumed that θ is related to the temperature at which the size of polar regions begins to expand rapidly [38].

Therefore, the most important conclusions from this part are connected with:

- connection between temperatures of characteristic anomalies of dielectric properties and evolution of temperature of polar areas,
- confirmation that crystal lattice defects increase the temperature at which polar regions disappear.

4. Perspectives

It has proved in this manuscript that occurrence of the intermediate phase in the antiferroelectric $PbZrO_3$ is related to the ratio of the donor to acceptor centers. This ratio is not in equilibrium, and centers being filled or emptied act similar to local stresses. Therefore, they influence local vibration of the crystal lattice. Because of small energy difference between the ferro- and antiferroelectric states, these defects—producing extra stresses in all $PbZrO_3$ sublattices—are also responsible for the intermediate phase appearance. Moreover, it was shown that in zirconium sublattice a local symmetry breaking also takes place. All those centers, being in different charge states, enhance the probability of phase coexistence.

However, even small amount of hetero-valent dopant on B-side, such as niobium, leads to extraordinary changes in electrical conductivity and phase transitions sequence. As has been already shown, new phase transition PZO single crystal doped with Nb can appear. Such dopant, depending on its concentration, must create or compensate defect so that to guarantee electrical neutrality of crystal. Therefore, mechanism of structural transformations in PZO:Nb crystal, including effect of coexistence of phases, seems to be much more complicated than in pure PZO. Investigations of the electron–phonon interactions in PZO:Nb would help to understand how to steer the properties of this functional antiferroelectric material through hetero-valent doping. Therefore, it would be interesting to study electronic structure of doped PZO.

The ambient pressure XPS tests are very sufficient to perform electron structure and resonant photoemission studies on pure and niobium-doped PZO crystal. Also defected PZO single crystals could be measured since under ultrahigh vacuum (needed for experiment) new defects are created. This experiment would allow the investigation of electronic structure and valence band in neutral conditions for PZO samples (i.e., in oxygen reach atmosphere) through the resonant photoemission in the case of Pb, Zr, O, and Nb elements. It would also provide information about niobium (or other dopands) concentration and oxidation states which could be checked only using synchrotron radiation because of very small amount of Nb which is non-delectable by classical fixed energy XPS. This information would support recent investigation on the influence of electrical field on defects distribution in PZO doped with Nb. This experiment could also provide information on the depth profiles of elements and their oxidation states which would accomplish previous work.

With the obtained data from the experiment could answer some questions, such as "What is the Nb ion crystallographic site(s) in the perovskite ABO_3 structure", "Is the Nb ions distribution in the PZO lattice homogeneous or depends on the depth from the surface", "What kind of chemical structures the Nb may, if any, form on the crystal surface", "What is an electronic state of Zr ions in the surface and bulk of the pure and doped PZO crystal." All those answers would help in understanding electron–phonon interaction, and reasons of the intermediate phase's appearance in PZO. To the best of my knowledge this kind of information is not presented in the literature on the PZO crystal doped with foreign ions, even for so intensively studied famous PZT materials. In particular, the Zr ionic states in lead zirconate has not been discussed so far and because it was presented in this manuscript, it cannot be neglected.

Another important field which should be investigated, is crystal structure studied by synchrotron radiation and neutron diffraction. This would allow investigating subtle changes of crystal structure caused by doping and would bring essential information on intermediate phases' structure. Also, in the context of recent studies of the incommensurate phase occurring in $PbZrO_3$ and $PbHfO_3$, it may be interesting to examine thoroughly the intermediate phases in this respect. In particular, when time-dependent phase transitions observed in them were characteristic for modulated phases (commensurate or incommensurate). Studies by means of neutron diffraction allow observation of

subtle shifts of oxygen ions forming octahedrons. Those tilts of oxygen octahedrons are an important phenomenon accompanying phase transitions in this group of compounds. Such tilts, apart from the natural occurrence in PZO crystals, may be caused by defects in the crystal lattice occurring in each sublattices. Therefore, the key in further exploring the mechanism of phase transitions seems to be a thorough analysis of the impact of defects on the oxygen octahedron and lead ion shifts in the same on the phase transitions occurring in both doped and undoped PZO crystals.

5. Conclusions

The series of investigations presented provides a coherent picture of the impact of defects on the instability of crystal lattice vibrations in materials based on antiferroelectric $PbZrO_3$. The most important conclusions are the following ones:

- The electronic state of point defects in sublattices A, B, and O has a significant impact on the appearance of the so-called intermediate phase in $PbZrO_3$ below T_c. It has been shown that the defects in the zirconium sublattice, previously omitted in the literature, also influence the properties of $PbZrO_3$;
- admixture of niobium Nb^{5+} and bismuth Bi^{3+}, i.e., ions with a valence different from ion A and B in the structure $A^{2+}B^{4+}O^{2-}{}_3$, causes defects in the lead sublattice, leading to breaking of local symmetry at temperatures above T_{BH}, i.e., the temperature determined for pure perovskite compounds with ABO_3 structure;
- experimental confirmation has been provided of interrelation between acoustic and optical modes in $PbZrO_3$ predicted by theory, and indicating the presence of polar regions at temperatures above T_c.

Conflicts of Interest: The author declares no conflict of interest. The funders had no role in the design of the study; in the collection, analyses, or interpretation of data; in the writing of the manuscript, or in the decision to publish the results.

References

1. Müller, K.A.; Berlinger, W. Microscopic probing of order-disorder versus displacive behavior in $BaTiO_3$ by Fe^{3+} EPR. *Phys. Rev. B* **1986**, *34*, 6130–6136. [CrossRef] [PubMed]
2. Müller, K.; Berlinger, W.; Blazey, K.; Albers, J. Electron paramagnetic resonance of Mn^{4+} in $BaTiO_3$. *Solid State Commun.* **1987**, *61*, 21–25. [CrossRef]
3. Müller, K.A.; Fayet, J.C. *Structural Phase Transitions II*; Müller, K.A., Thomas, H., Eds.; Springer: Berlin/Heidelberg, Germany, 1991; pp. 1–82.
4. Comès, R.; Lambert, M.; Guinier, A. The chain structure of $BaTiO_3$ and $KNbO_3$. *Solid State Commun.* **1968**, *6*, 715–719. [CrossRef]
5. Ravel, B.; Stern, E.A.; Vedrinskii, R.I.; Kraizman, V. Local structure and the phase transitions of $BaTiO_3$. *Ferroelectrics* **1998**, *206*, 407–430. [CrossRef]
6. Zalar, B.; Laguta, V.V.; Blinc, R. NMR Evidence for the coexistence of order-disorder and displacive components in barium titanate. *Phys. Rev. Lett.* **2003**, *90*, 37601. [CrossRef] [PubMed]
7. Zalar, B.; Lebar, A.; Seliger, J.; Blinc, R.; Laguta, V.V.; Itoh, M. NMR study of disorder in $BaTiO_3$ and $SrTiO_3$. *Phys. Rev. B* **2005**, *71*, 064107. [CrossRef]
8. Chaves, A.S.; Barreto, F.C.S.; Nogueira, R.A.; Zẽks, B. Thermodynamics of an eight-site order-disorder model for ferroelectrics. *Phys. Rev. B* **1976**, *13*, 207–212. [CrossRef]
9. Völkel, G.; Muller, K.A. Order-disorder phenomena in the low-temperature phase of $BaTiO_3$. *Phys. Rev. B* **2007**, *76*, 094105. [CrossRef]

10. Geneste, G.; Kiat, J.-M. Ground state of ca-doped strontium titanate: Ferroelectricity versus polar nanoregions. *Phys. Rev. B* **2008**, *77*, 174101. [CrossRef]

11. Ziębińska, A.; Rytz, D.; Szot, K.; Górny, M.; Rolder, K. Birefringence above T_c in single crystals of barium titanate. *J. Phys. Condens. Matter* **2008**, *20*, 142202. [CrossRef]

12. Ko, J.-H.; Kojima, S.; Koo, T.-Y.; Jung, J.H.; Won, C.J.; Hur, N. Elastic softening and central peaks in $BaTiO_3$ single crystals above the cubic-tetragonal phase-transition temperature. *Appl. Phys. Lett.* **2008**, *93*, 102905. [CrossRef]

13. Tai, R.Z.; Namikawa, K.; Sawada, A.; Kishimoto, M.; Tanaka, M.; Lu, P.; Nagashima, K.; Maruyama, H.; Ando, M. Picosecond view of microscopic-scale polarization clusters in paraelectric $BaTiO_3$. *Phys. Rev. Lett.* **2004**, *93*, 087601. [CrossRef] [PubMed]

14. Kwapuldński, J.; Pawełczyk, M.; Dec, J. Thermal vibrations in $PbTiO_3$ crystals. *Ferroelectrics* **1997**, *192*, 307–311. [CrossRef]

15. Kwapulinski, J.; Kusz, J.; Böhm, H.; Dec, J. Thermal vibrations in $PbTiO_3$ single crystals. *J. Phys. Condens. Matter* **2005**, *17*, 1825–1830. [CrossRef]

16. Kwapulinski, J.; Pawelczyk, M.; Dec, J. On the Pb thermal vibrations in $PbHfO_3$ crystals. *J. Phys. Condens. Matter* **1994**, *6*, 4655–4659. [CrossRef]

17. Bussmann-Holder, A.; Kim, T.H.; Lee, B.W.; Ko, J.-H.; Majchrowski, A.; Soszyński, A.; Roleder, K. Phase transitions and interrelated instabilities in $PbHfO_3$ single crystals. *J. Phys. Condens. Matter* **2015**, *27*, 105901. [CrossRef]

18. Bussmann-Holder, A.; Ko, J.-H.; Majchrowski, A.; Górny, M.; Roleder, K. Precursor dynamics, incipient ferroelectricity and huge anharmonicity in antiferroelectric lead zirconate $PbZrO_3$. *J. Phys. Condens. Matt.* **2013**, *25*, 212202. [CrossRef]

19. Tennery, V.J. A study of the phase transitions in $PbZrO_3$. *J. Electrochem. Soc.* **1965**, *112*, 1117. [CrossRef]

20. Tennery, V.J. High-temperature phase transitions in $PbZrO_3$. *J. Am. Ceram. Soc.* **1966**, *49*, 483–486. [CrossRef]

21. Goulpeau, L. Phase Transitions in Lead Zirconate. *Sov. Phys. Solid State* **1967**, *8*, 1970–1971.

22. Scott, B.A.; Burns, G. Crystal growth and observation of the ferroelectric phase of $PbZrO_3$. *J. Am. Ceram. Soc.* **1972**, *55*, 331–333. [CrossRef]

23. Ujma, Z.; Hańderek, J. Phase transitions and spontaneous polarization in $PbZrO_3$. *Phys. Status Solidi (a)* **1975**, *28*, 489–496. [CrossRef]

24. Whatmore, R.W.; Glazer, A.M. Structural phase transitions in lead zirconate. *J. Phys. C Solid State Phys.* **1979**, *12*, 1505. [CrossRef]

25. Roleder, K.; Dee, J. The defect-induced ferroelectric phase in thin $PbZrO_3$ single crystals. *J. Phys. Condens. Matter* **1989**, *1*, 1503–1510. [CrossRef]

26. Ujma, Z.; Hańderek, J. The influence of defects in the Pb and O sub-lattices on dielectric properties and phase transitions in $PbZrO_3$. *Phase Transit.* **1983**, *3*, 121–130. [CrossRef]

27. Ujma, Z. Dielectric properties and phase transitions in $PbZrO_3$ with oxygen vacancies. *Phase Transit.* **1984**, *4*, 169–181. [CrossRef]

28. Ujma, Z.; Dmytrow, D.; Handerek, J. The intermediate ferroelectric phase in $PbZrO_3$ with high concentration of defects. *Ferroelectrics* **1988**, *81*, 107–110. [CrossRef]

29. Ko, J.-H.; Górny, M.; Majchrowski, A.; Roleder, K.; Bussmann-Holder, A. Mode softening, precursor phenomena, and intermediate phases in $PbZrO_3$. *Phys. Rev. B* **2013**, *87*, 184110. [CrossRef]

30. Bussmann-Holder, A.; Beige, H.; Völkel, G. Precursor effects, broken local symmetry, and coexistence of order-disorder and displacive dynamics in perovskite ferroelectrics. *Phys. Rev. B* **2009**, *79*, 184111. [CrossRef]

31. Kajewski, D.; Kubacki, J.; Balin, K.; Lazar, I.; Piecha, J.; Bussmann-Holder, A.; Ko, J.-H.; Roleder, K. Defect-induced intermediate phase appearance in a single $PbZrO_3$ crystal. *J. Alloys Compd.* **2020**, *812*, 152090. [CrossRef]

32. Kajewski, D.; Ujma, Z.; Zajdel, P.; Roleder, K. Nb-stabilized locally broken symmetry below and above T_c in a $PbZrO_3$ single crystal. *Phys. Rev. B* **2016**, *93*, 054104. [CrossRef]

33. Kajewski, D.; Zajdel, P.; Sitko, R.; Lazar, I.; Bussmann-Holder, A.; Ko, J.-H.; Roleder, K.; Roleder, R. Defect induced lattice instabilities and competing interactions in niobium doped lead zirconate single crystals. *J. Alloys Compd.* **2018**, *739*, 499–503. [CrossRef]

34. Kajewski, D.; Jankowska-Sumara, I.; Ko, J.-H.; Lee, J.W.; Majchrowski, A.; Bussmann-Holder, A.; Roleder, K. Influence of Nb^{+5} ions on phase transitions and polar disorder above T_c in $PbZrO_3$ studied by Raman spectroscopy. *J. Am. Ceram. Soc.* **2020**, *103*, 3657–3666. [CrossRef]

35. Kajewski, D.; Ko, J.-H.; Lee, J.W.; Jankowska-Sumara, I.; Majchrowski, A.; Bussmann-Holder, A.; Roleder, K. Phase coexistence in slightly doped $PbZrO_3$ investigated by brillouin light scattering. In Proceedings of the 5th International Conference on Advanced Electromaterials, Jeju, Korea, 5–8 November 2019.

36. Kajewski, D.; Ko, J.-H.; Lee, J.W.; Jankowska-Sumara, I.; Majchrowski, A.; Roleder, K. Isothermal self-ordering in niobium doped lead zirconate single crystals. In Proceedings of the European Meeting on Ferroelectricity, Lausanne, Switzerland, 14–19 June 2019.

37. Kajewski, D.; Kubacki, J.; Bussmann-Holder, A.; Roleder, K. Surface–bulk interrelation in a $PbZrO_3$ single crystal. *J. Mater. Chem. C* **2017**, *5*, 10456–10461. [CrossRef]

38. Kajewski, D.; Zajdel, P.; Soszyński, A.; Koperski, J.; Lazar, I.; Roleder, K. Bismuth doped $PbZr_{0.70}Ti_{0.30}O_3$ ceramics and their properties driven by high temperature local polarity. *Ceram. Int.* **2019**, *45*, 9871–9877. [CrossRef]

39. Wojcik, K.; Ujma, Z. Nonstoichiometry and optical absorption in $PbZrO_3$ and $PbTiO_3$ single crystals. *Ferroelectrics* **1989**, *89*, 133–142. [CrossRef]

40. Ujma, Z.; Dmytrow, D.; Pawełczyk, M. Structure and electrical properties of $PbZrO_3$ doped with Nb_2O_5. *Ferroelectrics* **1991**, *120*, 211–224. [CrossRef]

41. Shirane, G.; Sawaguchi, E.; Takeda, A. On the phase transition in lead zirconate. *Phys. Rev.* **1950**, *80*, 485. [CrossRef]

42. Vales-Castro, P.; Roleder, K.; Zhao, L.; Li, J.; Kajewski, D.; Catalan, G. Flexoelectricity in antiferroelectrics. *Appl. Phys. Lett.* **2018**, *113*, 132903. [CrossRef]

43. Vales-Castro, P.; Faye, R.; Vellvehí, M.; Perpinya, X.; Kajewki, D.; Roleder, K.; Defay, E.; Perez-Tomas, V.; Catalan, G. Direct measurement of large negative and positive electrocaloric effects in antiferroelectric $PbZrO_3$, advanced materials. *Sci. Adv.* **2020**. submitted for publication.

44. Benguigui, L. Ferroelectricity and antiferroelectricity in pure and Nb_2O_5 doped lead zirconate. *J. Solid State Chem.* **1971**, *3*, 381–386. [CrossRef]

45. Samara, G.A. Pressure and temperature dependence of the dielectric properties and phase transitions of the antiferroelectric perovskites: $PbZrO_3$ and $PbHfO_3$. *Phys. Rev. B* **1970**, *1*, 3777–3786. [CrossRef]

46. Ujma, Z.; Hańderek, J. Electric Properties of $PbZrO_3$ monocrystals. *Acta Phys. Polon. A* **1978**, *53*, 665.

47. Ujma, Z.; Hańderek, J. Space-charge polarization and phase transitions in lead zirconate. *Phase Transit.* **1980**, *1*, 363–376. [CrossRef]

48. Frantti, J.; Fujioka, Y.; Puretzky, A.A.; Xie, Y.; Ye, Z.-G.; Glazer, A.M. A statistical model approximation for perovskite solid-solutions: A Raman study of lead-zirconate-titanate single crystal. *J. Appl. Phys.* **2013**, *113*, 174104. [CrossRef]

49. Burkovsky, R.G.; Bronwald, Y.A.; Filimonov, A.V.; Rudskoy, A.I.; Chernyshov, D.; Bosak, A.; Hlinka, J.; Long, X.; Ye, Z.-G.; Vakhrushev, S. Structural heterogeneity and diffuse scattering in morphotropic lead zirconate-titanate single crystals. *Phys. Rev. Lett.* **2012**, *109*, 097603. [CrossRef] [PubMed]

50. Phelan, D.; Long, X.; Xie, Y.; Ye, Z.-G.; Glazer, A.M.; Yokota, H.; Thomas, P.; Gehring, P.M. Single crystal study of competing rhombohedral and monoclinic order in lead zirconate titanate. *Phys. Rev. Lett.* **2010**, *105*, 207601. [CrossRef]

51. Lazar, I.; Kajewski, D.; Majchrowski, A.; Soszyński, A.; Koperski, J.; Roleder, K. A contribution to understanding the complex phase diagram of PZT compounds. *Ferroelectrics* **2016**, *500*, 67–75. [CrossRef]

52. Lazar, I.; Oboz, M.; Kubacki, J.; Majchrowski, A.; Piecha, J.; Kajewski, D.; Roleder, K. Weak ferromagnetic response in $PbZr_{1-x}Ti_xO_3$ single crystals. *J. Mater. Chem. C* **2019**, *7*, 11085–11089. [CrossRef]

53. Lazar, I.; Oh, S.H.; Ko, J.-H.; Zajdel, P.; Kajewski, D.; Majchrowski, A.; Piecha, J.; Koperski, J.; Soszyński, A.; Roleder, K. Additional phase transition in a $PbZr_{0.87}Ti_{0.13}O_3$ single crystal. *J. Phys. D Appl. Phys.* **2019**, *52*, 115302. [CrossRef]

54. Zhang, N.; Yokota, H.; Glazer, A.M.; Ren, Z.; Keen, D.A.; Keeble, D.S.; Thomas, P.A.; Ye, Z.-G. The missing boundary in the phase diagram of $PbZr_{1-x}Ti_xO_3$. *Nat. Comm.* **2014**, *5*, 5231. [CrossRef] [PubMed]

55. Geday, M.A.; Glazer, A.M. Birefringence of $SrTiO_3$ at the ferroelastic phase transition. *J. Phys. Condens. Matter* **2004**, *16*, 3303–3310. [CrossRef]

56. Wieczorek, K.; Ziebiniska, A.; Ujma, Z.; Szot, K.; Górny, M.; Franke, I.; Koperski, J.; Soszyński, A.; Roleder, K. Electrostrictive and piezoelectric effect in BaTiO$_3$ and PbZrO$_3$. *Ferroelectrics* **2006**, *336*, 61–67. [CrossRef]

57. Kim, J.H.; Choi, J.-Y.; Jeong, M.-S.; Ko, J.-H.; Ahart, M.; Ko, Y.H.; Kim, K.J. Development of a high-pressure brillouin spectrometer and its application to an ethylene-vinyl acetate copolymer. *J. Korean Phys. Soc.* **2012**, *60*, 1419–1423. [CrossRef]

58. Rietveld, H.M. A profile refinement method for nuclear and magnetic structures. *J. Appl. Crystallogr.* **1969**, *2*, 65–71. [CrossRef]

59. Rodriguez-Carvajal, J. Recent developments of the program FULLPROF commission on powder diffraction. *IUCr Newsl.* **2001**, *26*, 12–19.

60. Waghmare, U.V.; Rabe, K.M. Lattice instabilities, anharmonicity and phase transitions in PbZrO$_3$ from first principles. *Ferroelectrics* **1997**, *194*, 135–147. [CrossRef]

61. Singh, D.J. Structure and energetics of antiferroelectric PbZrO$_3$. *Phys. Rev. B* **1995**, *52*, 12559–12563. [CrossRef]

62. Kagimura, R.; Singh, D.J. First-principles investigations of elastic properties and energetics of antiferroelectric and ferroelectric phases of PbZrO$_3$. *Phys. Rev. B* **2008**, *77*, 104113. [CrossRef]

63. Dai, X.; Li, J.; Viehland, D. Weak ferroelectricity in antiferroelectric lead zirconate. *Phys. Rev. B* **1995**, *51*, 2651–2655. [CrossRef]

64. Roleder, K.; Maglione, M.; Fontana, M.D.; Dec, J. Behaviour of a polar relaxation mode around the phase transition point in the antiferroelectric single crystal. *J. Phys. Condens. Matter* **1996**, *8*, 10669–10678. [CrossRef]

65. Aoyagi, S.; Kuroiwa, Y.; Sawada, A.; Tanaka, H.; Harada, J.; Nishibori, E.; Takata, M.; Sakata, M. Direct observation of covalency between O and disordered Pb in cubic PbZrO$_3$. *J. Phys. Soc. Jpn.* **2002**, *71*, 2353–2356. [CrossRef]

66. Jankowska-Sumara, I.; Jeong, M.-S.; Ko, J.-H.; Majchrowski, A.; Zmija, J. Phase transitions in PbZr$_{0.72}$Sn$_{0.28}$O$_3$ single crystals studied by Raman spectroscopy. *Phase Transit.* **2016**, *89*, 768–776. [CrossRef]

67. Hlinka, J.; Ostapchuk, T.; Buixaderas, E.; Kadlec, F.; Kužel, P.; Gregora, I.; Kroupa, J.; Savinov, M.; Klic, A.; Drahokoupil, J.; et al. Multiple soft-mode vibrations of lead zirconate. *Phys. Rev. Lett.* **2014**, *112*. [CrossRef]

68. Ostapchuk, T.; Petzelt, J.; Zelezny, V.; Kamba, S.; Bovtun, V.; Porokhonskyy, V.; Pashkin, A.; Kužel, P.; Glinchuk, M.D.; Bykov, I.P.; et al. Polar phonons and central mode in antiferroelectric PbZrO$_3$ ceramics. *J. Phys. Condens. Matter* **2001**, *13*, 2677–2689. [CrossRef]

69. Pasto, A.E.; Condrate, R.A. Raman spectrum of PbZrO$_3$. *J. Am. Ceram. Soc.* **1973**, *56*, 436–438. [CrossRef]

70. Rodenbücher, C.; Speier, W.; Bihlmayer, G.; Breuer, U.; Waser, R.; Szot, K. Cluster-like resistive switching of SrTiO$_3$: Nb surface layers. *New J. Phys.* **2013**, *15*, 103017. [CrossRef]

71. Pilch, M.; Molak, A.; Szot, K. Thermal treatment effects in PbTiO$_3$ crystals studied by XPS and electric conductivity tests. *Ferroelectrics* **2014**, *466*, 51–62. [CrossRef]

72. Szeremeta, A.; Pawlus, S.; Pilch, M.; Balin, K.; Leonarska, A.; Molak, A.; Paluch, M. Relaxor state and electric relaxations induced by the addition of Bi and Mn ions to Pb(Zr$_{0.70}$Ti$_{0.30}$)O$_3$ ceramics. *Ceram. Int.* **2017**, *43*, 11699–11709. [CrossRef]